Short distance pollen movement in a wind-pollinated tree, *Quercus lobata* (Fagaceae)

Andrea R. Pluess [a,b], Victoria L. Sork [a,c,*], Brian Dolan [d], Frank W. Davis [e], Delphine Grivet [a,1], Kurt Merg [a,2], Jeanette Papp [f], Peter E. Smouse [g]

[a] Department of Ecology and Evolutionary Biology, University of California Los Angeles, Los Angeles, CA 90095-1606, USA
[b] Institute of Terrestrial Ecosystems, Swiss Federal Institute of Technology (ETH), 8092 Zurich, Switzerland
[c] Institute of the Environment, University of California Los Angeles, Los Angeles, CA 90095, USA
[d] Department of Biomathematics, University of California Los Angeles, Los Angeles, CA 90095, USA
[e] Donald Bren School of Environmental Science and Management, University of California Santa Barbara, CA 93106, USA
[f] Department of Human Genetics University of California Los Angeles, Los Angeles, CA 90095, USA
[g] Department of Ecology, Evolution and Natural Resources, Cook College, Rutgers University New Brunswick, NJ 08901, USA

ARTICLE INFO

ABSTRACT

Short distance pollen dispersal shapes the local genetic structure of plant populations and determines the opportunity for genetic drift and local selection. In this paper we focus on short distance dispersal (SDD) of pollen in a low-density stand of a savannah oak, *Quercus lobata* Née. Specifically, we are interested in the proportional contributions of pollen donors, the pollen dispersal kernel that describes local matings, the extent to which wind influences mating success, and the extent to which pollen sources vary within the large canopy of these trees. Using maximum likelihood paternity analysis, we assigned sires for 474 outcrossed progeny of five seed trees, representing 120 of 160 potential mating pairs within a 250 m radius of each focal tree (ca. 20 ha plots). We first established that the effective number of pollen donors for progeny with sires within the plot was about 10 individuals, with average weighted pollination distances of 114.1 m. We estimated 18.5% pollen immigration into the 20 ha plots. We next established that the SDD portion of the dispersal kernel is best described by the exponential power, inverse power, and Weibull functions, all that capture high local dispersal with steep decay. Two of these models suggest that long distance dispersal is abundant, represented by a fat tail, while the Weibull indicates depauperate long distance dispersal, represented by a thin tail. The addition of a directional component corresponding to the predominant wind axis had no meaningful impact on these models. Finally, we established that different parts of an individual tree canopy of *Q. lobata* sample from the same homogeneous pollen pool showing no bias towards pollen sources near that part of the canopy. Overall findings suggest low-density *Q. lobata* populations show steep decay of SDD. Policies and ordinances governing the amount of allowable tree removal of savannah oak populations should recommend the preservation of local clusters of adults, as well as some connectivity among clusters.

© 2009 Elsevier B.V. All rights reserved.

1. Introduction

Pollen movement has two important aspects that must be taken into account when conserving or managing tree populations at a local or regional scale: the local distribution of genotypes via short distance dispersal (SDD) and genetic connectivity across landscapes via long distance dispersal (LDD) (Sork and Smouse, 2006). Wright (1943, 1946) recognized that local dispersal could lead to population subdivision as an outcome of restricted propagule flow. The neighbourhood size (N_e), the effective number of randomly mating individuals in a population within an area defined by the scale of dispersal, is the entity of contemporary evolutionary processes. The size of the local pollen neighbourhood is influenced by the short distance part of the pollen dispersal curve. The shape of the dispersal kernel is critical, because the steeper it is, near the origin, the more near-neighbour matings will dominate the pollen pool. Meanwhile the fatness or thinness of the tail will indicate whether long distance dispersal is common or rare (Austerlitz

et al., 2004), which is relevant to long-term connectedness across an extended landscape. For contemporary evolutionary processes, short distance dispersal will represent the majority of pollination events and determine the opportunities for genetic drift and local adaptation. Thus, as we consider the rapidly changing environmental settings for contemporary populations created by landscape transformation and climate change, the issue of short-term microevolutionary processes, shaped by dispersal kernel over short distances, is particularly salient.

The profile of pollen dispersal reflects the fertilization success of nearby pollen sources and the resulting impact on the effective number of pollen donors (Austerlitz et al., 2004). Various mathematical relationships can be used to describe the dispersal curve (Clark et al., 1999; Nathan and Muller-Landau, 2000; Cain et al., 2003; Nathan et al., 2003; Austerlitz et al., 2004; Oddou-Muratorio et al., 2005; Klein et al., 2006), including the inverse power law (Gregory, 1968), the exponential family, the exponential power law (Clark, 1998), the Weibull family (Weibull, 1951; Tufto et al., 1997), and the geometric family (Austerlitz et al., 2004). Using genetic data, the neighbourhood model of Adams and Birkes (1991) and the later work of Burczyk et al. (2002) assume an exponential dispersal curve to estimate short distance dispersal and immigration. The initial pollen pool structure analysis modelled in TwoGener by Smouse et al. (2001) utilized a bivariate normal distribution, following the tradition of Wright's (1943) neighbourhood equations, and a later version of TwoGener implemented an exponential curve (Austerlitz and Smouse, 2001). Frequently, studies that use genetic information to model pollen flow will compare the parameters for several models (Austerlitz et al., 2004; Klein et al., 2006; Robledo-Arnuncio and Garcia, 2007). It is known that both the inverse power and exponential power models fit dispersal data reasonably well (Okubo and Levin, 1989). In general, the differences among the mathematical functions are how they model the slope of the curve at short distances and the thinness/fatness of their tail probabilities for long distances. The inverse power function, for example, can be more sensitive in detecting a fat tail (e.g. Wingen et al., 2007), while the Weibull is more likely to detect a thin tail (Austerlitz et al., 2004). Which of these mathematical functions is best for modelling the steepness of SDD near the origin remains an open question.

For wind-pollinated species, pollen flow might also be asymmetrical due to direction and velocity of the wind (Okubo and Levin, 1989; Di-Giovanni et al., 1996). Because this asymmetry increases the variance in dispersal, it could lead to an underestimate of dispersal (Austerlitz et al., 2007). Some studies have found a slight directional effect of pollination along the predominant wind vector (Shen et al., 1981; Burczyk and Prat, 1997), while other studies have observed directionality, but without a specified relationship to wind direction (Burczyk et al., 1996, 2004; Robledo-Arnuncio and Gil, 2005). Lian et al. (2001) found that female flowers on one side of the maternal tree were fertilized mainly from pollen donors from that direction, which suggests that pollen dispersal is influenced by the spatial distribution of local trees. In large populations, these spatial effects probably average out, but, as population size and density decline, local patchiness of adults could become more significant.

Here, we explore the dynamics of short distance pollen dispersal in a savannah population of *Quercus lobata* Née (valley oak) during the mast-fruiting year of 2002, when essentially all adult trees shed pollen and a majority produced acorns. We first assign paternity for progeny from five focal seed trees, evaluating all potential pollen donors within a 250 m radius of each focal tree, resulting in five approximately 20 ha plots, covering a total area of almost 60 ha. For each plot, we determine the number of pollen donors within the plot and estimate pollen inflow from outside the

250 m circles. We then examined pollen recruitment for local progeny, to determine the best pollen dispersal curve of four commonly used distance-decay functions (the exponential, exponential power, inverse power, and Weibull). To discern the best distance-decay model for SDD, we regressed mating success frequencies against inter-pair distances. We also tested whether the shape of the dispersal kernel was influenced by wind direction by including the angular direction from the assigned paternal to the maternal tree in each of the dispersal models. Finally, we investigated whether local mating patterns varied within the canopies of individual trees. If local pollen movement is non-random, then the different parts of the very large canopy crowns of *Q. lobata* adults might sample pollen from different trees. Based on the outcomes of the genetic analyses, we discuss the implications for sustainable management of valley oak.

2. Materials and methods

2.1. Study species and study site

Q. lobata Née (valley oak) is a diploid, wind-pollinated, monoecious, and predominantly outcrossing tree species (Sork et al., 2002a). It flowers in February through early April, before leaves emerge (V.L.S., personal observation). Each flower can produce one acorn. Seeds mature in late September to early November of the year of pollination. *Q. lobata* is endemic to California, occurring in savannah oak communities, oak woodlands, and riparian oak forests on deep loamy soils, principally below 600 m of elevation in the Central Valley, surrounding valleys, and foothills (Pavlik et al., 1991). *Q. lobata* defines the ecosystem it occupies and determines the biodiversity of that habitat, ranging from soil microbes to wildlife. Due to its proclivity to occupy locations that are desirable for farmlands, ranches, vineyards, and suburban developments, *Q. lobata* has lost more of its habitat than any other oak species in California. For example, in the San Joaquin Valley, the core area of its distribution, riparian valley oak woodland, has declined from 2335 km^2 in the pre-European settlement period to 109 km^2 in 2000 A.D., so that it now occupies ~5% of its historical range (Kelly et al., 2005). Two critical factors for long-term persistence of the valley oak ecosystem are loss of habitat, resulting in small, fragmented populations, and lack of demographic recruitment, leading to population thinning. The recruitment problems are caused by many factors, including herbivory by rodents, grazing by cattle and deer, and competition with European grasses, all of which have negative demographic consequences for oak populations (Tyler, 2006).

We conducted the study in the mixed oak savannah of Sedgwick Reserve (N 34°42′, W 120°02′), 10 km northeast of Santa Ynez (Santa Barbara County, CA, USA). Over the past 60 years, tree densities in oak savannahs and woodlands have declined here by nearly 20%, due to a combination of tree mortality and the absence of new recruitment (Mahall et al., 2005). The study trees are located along the valley floor and the adjacent slopes of Figueroa Creek and grow interspersed with *Quercus agrifolia* and *Quercus douglasii* (Fig. 1). The *Q. lobata* stem density in the vicinity of the sampled seed trees is 1.7 adult trees/ha. Adults are usually greater than 40 cm in stem diameter at breast height, with crown areas of 64.5–581.9 m^2 (291.6 m^2 ± 129 SD), and crown diameters that can range from 10 to 30 m.

During the flowering period of the year under study, hourly anemometer data were collected 900 m from the centre of our study site at the weather station managed by Sedgwick Reserve. Our analysis of these data shows strong directionality from the west-northwest (290°) and wind speeds often exceeding 3.5 m/s (Fig. 2). This speed is equivalent to ca. 7 knots, typical of the upper Santa Ynez Valley (Ogden, 1975).
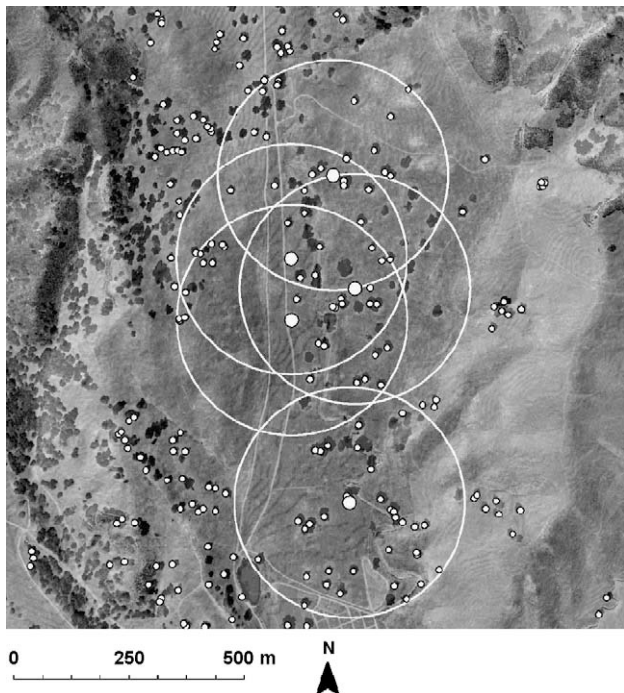
Fig. 1. Map of the five focal *Quercus lobata* seed trees and the surrounding landscape. The seed tree is in the centre of each circular buffer area with radius of 250 m. All conspecific adults are marked with a white dot.

2.2. Sampling

In the fall of 2002, we selected five maternal trees with similar crown sizes (365.1 m^2 ± 30.5 SD) and large crops of emerging acorns (adult ID's: 32, 35, 165, 844, and 889). These trees are located in the centre of the study site and at least 500 m from the edge of our mapped and genotyped adult population. In September, we bagged branches with approximately the same numbers of emerging acorns on the four directional sides of each tree crown. Fallen ripe acorns remained in the bag until collection in November. Acorns were stored in moist bags in the dark at 10 °C until they were planted in December
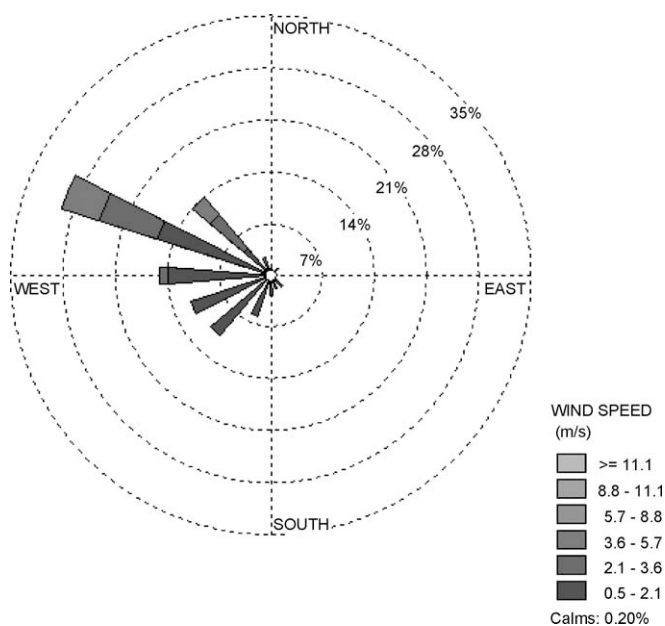

Fig. 2. Wind-rose describing the direction and velocity frequency of wind during the main flowering period of the study year 2002 between 10 am and 6 pm.

2002. We collected seedling leaf tissue in January 2003, and stored the tissue at −80 °C, pending genetic analysis.

For each focal seed tree, we identified and genotyped all (but one that was inadvertently mislabelled) candidate paternal trees within a 250 m buffer of 19.6 ha each, which we will refer to as 20 ha plots. The radius of the buffer is approximately twice as large as the indirectly assessed average effective pollen dispersal distance of 120 m estimated for this same population in 2001 (Austerlitz et al., 2004). The distances between focal seed trees ranged from 132 to 711 m, and as a result of overlapping neighbourhoods, the total area under study was 58.9 ha (Fig. 1).

2.3. Laboratory methods

We extracted DNA from adults and progeny, using 30–40 mg frozen leaf tissue per specimen, which was ground in tubes with a tungsten ball (Mixer Mill MM301, Retsch, Haan, Germany), following the cetyltrimethylammonium bromide (CTAB) method described in Sork et al. (2002b). Some samples with low DNA amplification were re-extracted with the DNeasy Plant Mini Kit (Qiagen, Valencia, USA) to reduce the amount of secondary plant components. We amplified seven nuclear microsatellite loci (i.e., SSR: Simple Sequence Repeats): MSQ4 (Dow et al., 1995), QpZAG1/5, QpZAG9, QpZAG36, QpZAG110 (Steinkellner et al., 1997), QrZAG11, and QrZAG20 (Kampfer et al., 1998). Amplification were carried out in 8 μl reaction mixture containing ca. 20 ng DNA, four dNTPs (each 0.4 mM), 0.6 μM primer, adjusted concentrations of MgCl$_2$ for each primer (2.5 mM for QpZag36; 3.0 mM for QpZAG110; 3.5 mM for MSQ4; 6.5 mM for QpZAG1/5, QpZag9, QrZag11, and QrZAG20), 1× Taq polymerase buffer, 0.75 mg/ml of Bovine Serum Albumin, and 0.5 unit of Taq polymerase (AmpliTaq Gold, AppliedBioSystems, Foster City, CA, USA). The reaction cycle consisted of an initial denaturing of 12 s at 95 °C, followed by 17 cycles of 30 s denaturing at 94 °C, 1 min annealing from 66 °C to 50 °C (Dow et al., 1995; Steinkellner et al., 1997; Kampfer et al., 1998), and 45 s extension at 72 °C, followed by 19 cycles of 30 s denaturing at 89 °C, 1 min annealing at 50 °C, and 45 s extension at 72 °C, with a final extension step of 72 °C for 3 min. A negative PCR control (PCR mixture without DNA) was included in each run to check for contamination. In addition to the ABI standard, two standard samples were included in each run for further calibration in the subsequent fragment length analyses. We measured the length of the amplified sequence on an ABI 3700 capillary sequencer at the UCLA Sequencing & Genotyping Core Facility (http://www.genetics.ucla.edu/sequencing/index.php).

Raw data were analyzed with the ABI Genotyper software to assign alleles to bins. Repeatability was evaluated and confirmed by re-genotyping one-third of all loci, after repeating the PCR reactions.

2.4. Paternity analysis

To assign pollen donors, we used the software CERVUS, based on the maximum likelihood method (Marshall et al., 1998). CERVUS allows the assignment of paternity at different confidence levels (CL) and, like many studies, we report both the 80% CL and 95% CL. The 80% CL ensures an assignment of a larger number of offspring with a higher probability of Type I errors, while the 95% CL is less likely to assign the wrong paternal candidate, but may miss pollination events due to its higher probability of Type II errors. CERVUS categorically assigns paternity to a particular candidate paternal tree if the difference (Δ) in the likelihoods of the most likely candidate and the second most likely candidate exceeds a certain threshold of Δ (Meagher, 1986). This threshold is determined via computer simulation of paternity inferences. For paternity assignment, our dataset included 840 progeny with at

least five of the seven loci. For the simulation (10,000 cycles), we used the allele frequencies of all adult trees ($N = 306$) in Figueroa Creek Valley (ca. 200 ha), along with the following parameters: 39 candidate paternal trees, 85% of candidate paternal trees sampled, 90.6% of loci typed, and 1% of loci mistyped.

The simulation parameters and confidence levels are critical to the determination of a significant threshold score for Δ, and Δ is affected by how CERVUS is run. First, for continuous populations, it is always difficult to gauge *a priori* the level of incoming pollen from outside the plot area. Based on analyses of this population for the 2001 fruiting season (Austerlitz et al., 2004), we expected immigration to be about 15%. This setting does not preclude estimating higher levels of gene flow than 15%. Second, the paternity analysis was restricted to paternal candidates within the 250 m radius buffers, because this area maximized our ability to make paternal assignment. When plot area increases, the number of potential candidates also increases, which makes it difficult to assign pollen donors. Third, based on seven loci, we allowed up to two mismatches between progeny, potential pollen donor and maternal tree, as long as the "best candidate" was within the 80% or 95% confidence limit. Given that we had some genotyping error due to null alleles, mutations, and detection errors, this setting avoids overestimation of pollen inflow (Slavov et al., 2005) while maximizing paternal assignment (Oddou-Muratorio et al., 2003). Offspring that lack assignment were classified into two groups. The unassigned progeny with multiple candidate donors and zero or one mismatch with the maternal and the best paternal tree was counted as pollen movement within the plot. The remainder of unassigned progeny had several mismatches and were therefore considered as pollen flow events. Cryptic gene flow was calculated based on the exclusion probability of potential paternal candidates: number of assigned offspring $\times$ [1 − (exclusion probability)$^{33.2}$] (Westneat and Webster, 1994). The percentages of cryptic gene flow were estimated in relation to all genotyped offspring.

2.5. Summary of mating patterns

For each focal seed tree, we calculated the number of candidate pollen donors, the number of observed pollen donors and the effective number of pollen donors (N_{ep}) within the 250 m radius. N_{ep} was calculated, based on the relative contributions, including self-fertilization, of individual pollen donors in the 80% CL dataset, using the bias-corrected estimator $N_{ep} = (n-1)^2/\{\sum_i p_i^2 \cdot (n+1) \cdot (n-2) + (3-n)\}$ for the per maternal tree estimates, as well as for an overall estimate (Nielsen et al., 2003). These N_{ep} estimates reflect matings within the plot. We also estimated an adjusted N_{ep} that included the contributions of immigrant pollen by assuming that every pollen flow event comes from a separate pollen donor beyond the plot boundary. This assumption biases N_{ep} upwardly.

2.6. Modelling pollen dispersal

We modelled the observed frequencies of offspring per mating pairs (Y) as a function of inter-mate distances (X), using exponential, exponential power, inverse power, and Weibull functions (see Table 1 for the equations, which are taken from Klein et al., 2006). The frequencies per mating pair were the number of progeny assigned to a specific mating pair out of total progeny for that seed tree. Depending on the shape parameter (b), the chosen models represent different potentials for LDD (Clark, 1998). Thin-tailed functions, indicating low potential for LDD, decrease faster than the exponential function and are represented in the exponential power and Weibull models with $b > 1$. The exponential power and the Weibull functions with $b = 1$ reduce to the exponential model (Klein et al., 2006). The fat-tailed functions

Table 1

Functions used to fit distance (d) and direction (α) on the observed proportions of offspring per mating pairs. For all functions, the scale parameter (a) and shape parameter (b) are indicators of the distance effect and the coefficient (c) of the directional angle. Γ is the standard gamma function (Klein et al., 2006).

Dispersal families	Distance model	Combined model
Exponential[#]	$f_{\exp}(d) = \frac{a^2}{2\pi}\exp(-ad)$	$f(d,\alpha) = f_{\exp}(d) + c\alpha$
Exponential power[#]	$f_{epp}(d) = \frac{a^{2/b}b}{2\pi\Gamma(2/b)}\exp(-ad^b)$	$f(d,\alpha) = f_{epp}(d) + c\alpha$
Inverse power	$f_{pow}(d) = \frac{a}{d^b}$	$f(d,\alpha) = f_{pow}(d) + c\alpha$
Weibull[#]	$f_{wei}(d) = \frac{ab}{2\pi}d^{b-2}\exp(-ad^b)$	$f(d,\alpha) = f_{wei}(d) + c\alpha$

[#] Expression of distance models after Klein et al. (2006).

indicate high potential for LDD and decrease slower than an exponential function; they are represented by the exponential power and Weibull model with $b < 1$ or the inverse power model with $b < 2$ (see Appendix A).

To fit the different models to the paternity data, we used the nonlinear least squares (*nls*) routine in the statistical package R (Bates and Watts, 1988; Bates and Chambers, 1992). The resulting parameter estimates are inserted into the original distribution and the algorithm is iterated to convergence. We used the AIC index (Akaike, 1974) to evaluate goodness of fit. In comparing models, a smaller AIC (more negative) value indicates a better fit (Venables and Ripley, 2002).

To test whether wind directionality contributes significantly to the pollen dispersal curve, we added a variable representing directionality to the regression model. We estimated directionality as the angular offset of the mating pair axis from the main wind axis (west-northwest, 290°, with north = 0° and east = 90°). We also evaluated the angle between the mating pair, relative to the angle orthogonal to the wind axis (20°) as an alternative hypothesis, but when we found no significance, we did not pursue this alternative further. The angles between the tested direction and the identified pollen donors were transformed into a uniform distribution ranging between −1 and 1 by computing the arc tangent of the angular offset between the mating pair axis and the tested direction. This approach allows a linear, rather than sinusoidal, response to a change in the angle, and makes it easier to detect changes in angles near 0° and 180°.

2.7. Pollen mixing within a canopy

We performed two tests to determine whether different parts of the canopy reflect matings with different pollen sources. The first method was based on the paternity assignments. Here, we performed a χ^2 test of paternal heterogeneity, based on the location of an acorn within the crown and the directional quadrant of the assigned pollen donor with respect to proximity of the crown quadrant. The expected values were based on the numbers of paternity assignments of offspring in our 80% CL dataset, weighted by numbers of potential pollen donors in each quadrant. The sample size ($N = 379$) was slightly smaller than total number of assigned progeny because we only used acorns collected in the centre of the four quadrants of the canopies.

The second test assessed whether the pollen pool composition differs among canopy quadrants and among focal maternal trees, based on a hierarchical pollen pool structure analysis (Smouse et al., 2001). This test would detect genetic structure within an individual canopy, regardless of the direction. The sample included all progeny with no more than one missing locus out of the six most frequently expressed microsatellite loci ($N = 593$).

Table 2

Data of a maximum likelihood paternity analysis of offspring of five maternal trees based on assignments at 80% confidence level. Offspring are categorized as: likely self-fertilized; outcrossed and assigned to a candidate pollen source within plot; unassigned with multiple possible candidate pollen donors within plot; or pollen flow events with no candidate pollen source within plot (see text for details). N_{ep} is calculated using Nielsen et al.'s (2003) unbiased estimator. Average distance of effective pollen dispersal, d, was calculated for assigned, outcrossed progeny within plot.

Maternal tree ID	N_{seed}	N_{cp}	$N_{succ\ p}$	N_{ep}	$d \pm SD$ [m]	Selfed, assigned offspring	Outcrossed, assigned offspring	Multiple candidate pollen donors within plot	Pollen flow	Pollen flow adjusted N_{ep}
32	191	38	27	5.9	134.2 ± 59.2	0.0%	54.5%	25.1%	20.4%	11.3
35	123	33	24	13.3	151.3 ± 72.5	9.8%	46.3%	19.5%	24.4%	27.6
165	213	34	32	11.8	120.1 ± 67.2	1.9%	69.0%	17.4%	11.7%	16.1
844	187	30	20	9.2	68.5 ± 62.5	6.4%	52.4%	28.3%	12.8%	13.7
889	126	30	21	17.6	105.2 ± 64.0	0.8%	54.0%	15.9%	29.4%	41.9
Average $\pm$ SD	168.0 ± 40.9	33.2 ± 3.4	24.8 ± 4.9	$10.1^* \pm 4.7$	114.1 ± 64.0	$3.8\% \pm 4.2$	$55.2\% \pm 8.4$	$21.2\% \pm 5.3$	$19.7\% \pm 7.5$	$17.6^* \pm 13.7$
Total	840	92	83	32.0		3.5%	56.4%	21.7%	18.5%	56.9

Abbreviations: N_{seed}, number of seeds; N_{cp}, number of paternal candidates; $N_{succ\ p}$, number of successful paternal candidates; N_{ep}, unbiased effective male population size based on assigned offspring; d, average pollen dispersal distance of outcrossed, assigned offspring; pollen flow adjusted N_{ep}, unbiased N_{ep} based on assigned offspring plus pollen flow where for the latter it is assumed, that each offspring was sired by another paternal tree.

* Harmonic mean of N_{ep}.

3. Results

3.1. Patterns of paternity

The analysis of allele frequencies, required for the paternity analysis with CERVUS, was based on adult trees with genotypic information for at least five of the seven loci ($N = 306$). All loci were highly variable, with 8–22 alleles each, summing up to a total of 95 alleles. The observed and expected heterozygosity were 0.696 (±0.089 SD) and 0.721 (±0.118 SD), respectively. Accumulated over all seven loci, the allele frequencies yielded a paternal exclusion probability of 0.997, although, like all studies, this value over-estimates the probability, because the calculation assumes random mating and no spatial component.

Within the 250 m radius surrounding each focal seed tree were 30–38 potential pollen donors and a net total of 92 potential pollen donors for the entire dataset, resulting in 165 possible mating pairs (160 potential mating pairs, if selfing is excluded). For the 80% CL dataset, the average number of successful pollen donors was 24.8 (±4.9 SD) per focal tree (Table 2), and, for the 95% CL, it was 10.8 (±4.9 SD) per focal tree. Results of the paternity analysis indicated overall selfing rates of 3.5% per focal tree (Table 2), which is much

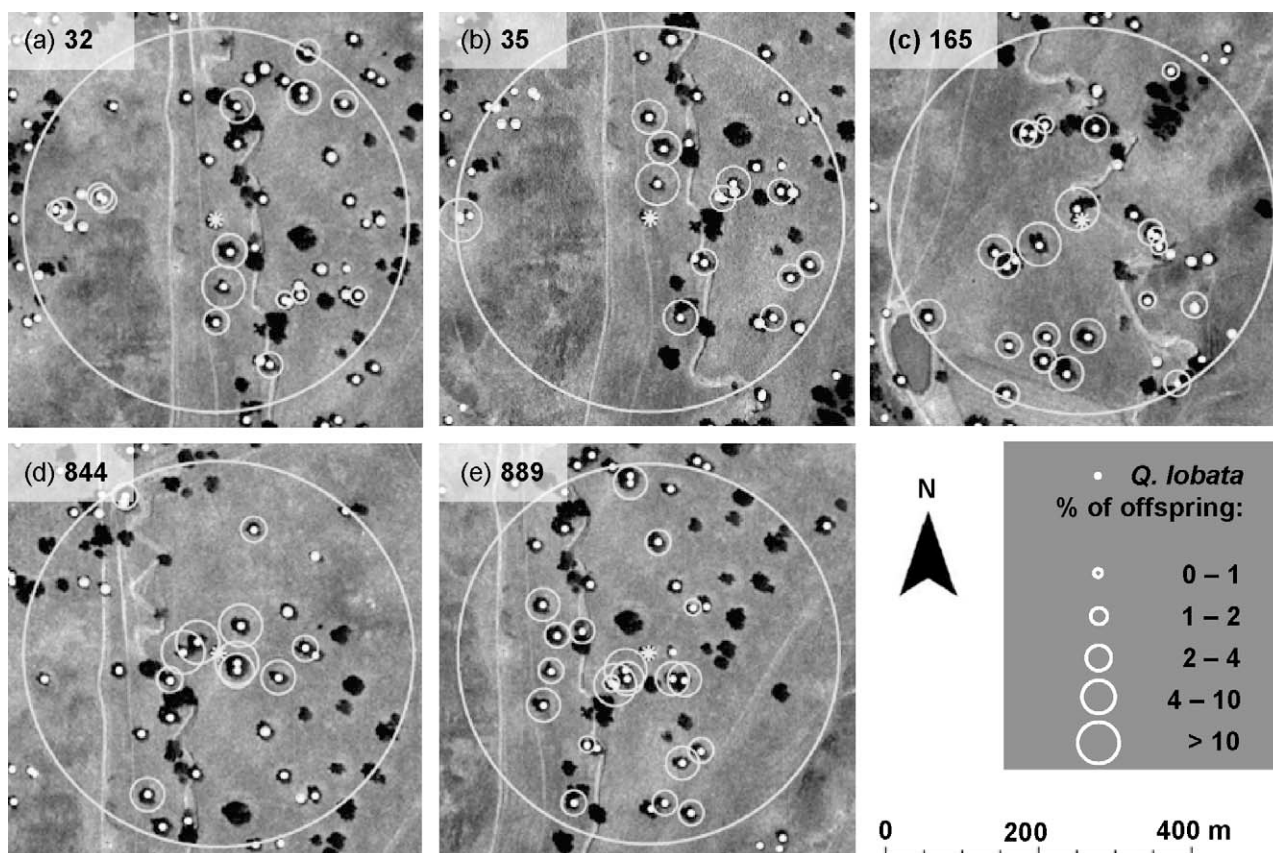**Fig. 3.** (a–e) Individual maps of the five *Quercus lobata* focal seed trees (*) in the centre of the 250 m radius plots. Conspecific adults are marked with a white dot, and contributing pollen donors are marked with an additional hollow circle where the diameter is approximately proportional to number of progeny sired. The dataset was generated with a maximum likelihood paternity assignment based on the 80% confidence level.

higher than the 0.5% selfing observed in the 95% CL dataset. The overall estimates of pollen-mediated gene flow into the 20 ha plots was 18.5% (Table 2), which may be an overestimate because the CERVUS results also indicated that every progeny included a possible candidate pollen donor within the plot despite occasional mismatches. We estimated cryptic gene flow for the 80% CL dataset of assigned progeny to be 5.7%. Because the gene flow frequency of 18.5% is probably an overestimate as pointed out above, the inclusion of cryptic gene flow to our estimate of pollen inflow is likely to inflate that estimate further. We identified unique pollen sources for 474 outcrossed progeny for the 80% CL data (or 56.4%, Table 2) and 164 outcrossed progeny for the 95% CL (or 19.5%). The remaining portions represent selfed progeny or progeny with more than one possible pollen parent. Patterns of mating varied spatially among the focal trees (Fig. 3a–e). Of the progeny with a unique sire, the most successful pollen donor sired 13.2–39.4% of the offspring per focal tree. For each focal seed tree, 1–3 pollen donors were responsible for more than 30% of the progeny, while the majority of the successful pollen donors sired only 1–2 offspring each (Fig. 3a–e).

Mean observed pollen dispersal distance of outcrossed progeny with mating pairs within the 250 m radius plot was 114.1 m ($\pm$64.0 SD, N = 474) for the 80% CL dataset (Table 2). This average distance is essentially a weighted mean because it is influenced by multiple progeny per mating pair. Since it is based on progeny with assigned parents only, it is best viewed as the one for the SDD component of the distribution, our primary target here.

Using the assignments based on the 80% CL dataset, we estimated the average effective number of pollen donors per focal trees and overall. The average N_{ep} for assigned progeny was 10.1 ($\pm$4.7 SD) individuals and adjusting the estimate for pollen inflow increases N_{ep} to 17.6 ($\pm$13.7 SD) individuals per focal tree (Table 2). For the ca. 60 ha area of the valley covered by the focal trees, the overall N_{ep} is about 32 individuals for assigned progeny and about 57 individuals after adjusting for pollen inflow (Table 2). Both estimates are less than the additive values of N_{ep} per maternal tree because of overlaps in the assigned pollen sources.

3.2. Modelling pollen dispersal

The pollen dispersal curve was fitted to frequencies of 124 mating pairs across five focal trees and 503 assigned offspring in the 80% CL dataset and 54 mating pairs for the 168 assigned offspring in the 95% CL dataset. All four models showed a significant distance effect and both sets of paternal allocations yielded the same pattern (Table 3, Fig. 4a and b). The exponential power, inverse power, and Weibull functions showed strong decay rates at short distances and the exponential model showed the weakest fit. The 80% CL and 95% Cl datasets revealed similar statistical trends, and for both datasets, the exponential power model had a slightly better fit to the data.

The fatness or thinness of the tail is indicated by the shape parameter, b. Our analyses showed $b < 1$ for the inverse power and exponential power models, which indicates a fat tail for pollen flow beyond the 250 m, and the lower the value the less thick the tail. In contrast, $b > 1$ for the Weibull function suggests a thin tail. Visually, the latter and the inverse power function are nearly indistinguishable within the 250 m buffer (Fig. 4a and b), but their shape parameters predict fat tails for the inverse power as well as the exponential power functions, and a thin tail for the Weibull function. If we compare the slope parameters of the 80% and 95% datasets, we see that the 95% CL dataset with more certain paternity has slightly thinner tails. For example, in the exponential power (distance only) models, b = 0.385 is less b = 0.440 for the 95% and 80% CL datasets, respectively. In the absence of detailed distance data on the pollen donors far beyond 250 m, there is no real way to assess or contrast those different tail assertions.

Table 3

Parameter estimates and Akaike (AIC) criteria for the distance models and combined (distance + wind angle) models. Parameters are the same as in Table 1. Significance values indicate the level of confidence in the parameter estimates and AIC values indicate the goodness of fit of the model. Models are shown for the 80% and 95% confidence level (CL) assignments.

Model parameters	a	b	c	AIC
80% CL (N = 124 parent pairs, 503 progeny)				
Exponential				
Distance	0.383***			−761.3
Distance + angle	0.287***		0.004 ns	−745.3
Exponential power				
Distance	1.715***	0.440***		−777.3
Distance + angle	1.694***	0.445***	0.006 ns	−778.6
Inverse power				
Distance	0.014***	0.240***		−764.1
Distance + angle	0.014***	0.237***	0.005 ns	−764.5
Weibull				
Distance	0.052***	1.768***		−765.0
Distance + angle	0.054***	1.770***	0.005 ns	−765.4
95% CL (N = 54 parent pairs, 168 progeny)				
Exponential				
Distance	0.204***			−978.5
Distance + angle	0.172***		0.004 ns	−975.8
Exponential power				
Distance	1.588*	0.385***		−984.9
Distance + angle	1.561*	0.391***	0.004*	−988.1
Inverse power				
Distance	0.005***	0.206*		−978.3
Distance + angle	0.005***	0.203*	0.004*	−980.6
Weibull				
Distance	0.017***	1.798***		−978.4
Distance + angle	0.018***	1.800***	0.004*	−980.8

ns = non-significant.
* $P < 0.05$.
*** $P < 0.001$.

However, the comparison of the models shows that the initial decay of pollination probability is far too steep for the exponential to be an acceptable model, and the figures confirm that interpretation.

To identify the extent to which the prevailing wind vector influences the pollen kernel, we added the angular offset between the inter-parent axis and the predominant wind vector to the model. The directional angle was non-significant for the 80% CL, whereas it was mostly significant for the 95% CL dataset, but it improved the overall model fit of the latter only slightly (Table 3). Thus, despite a strong prevailing wind, the assumption of isotropy in distance models is reasonable.

We tested the robustness of these findings in two ways. We used two datasets based on different certainty of paternity and both indicated a similar shaped dispersal kernel. Second, we reran our analysis with mating pairs in the plot that produced zero offspring. Our reported models excluded these pairs because we could not be sure that such pairs were capable of reproducing. However, the inclusion of these mating pairs yielded the same statistical trends as report here: SDD's are steep and tails are fat for two models and thin for the Weibull function.

3.3. Pollen mixing within a canopy

The arrays of assigned pollen donors of progeny did not differ among the four quadrants within seed tree canopies. The χ^2-analysis showed no significant heterogeneity, summed over the five maternal trees (χ^2 = 45.8, df = 45, N = 379, $P > 0.1$) and none of
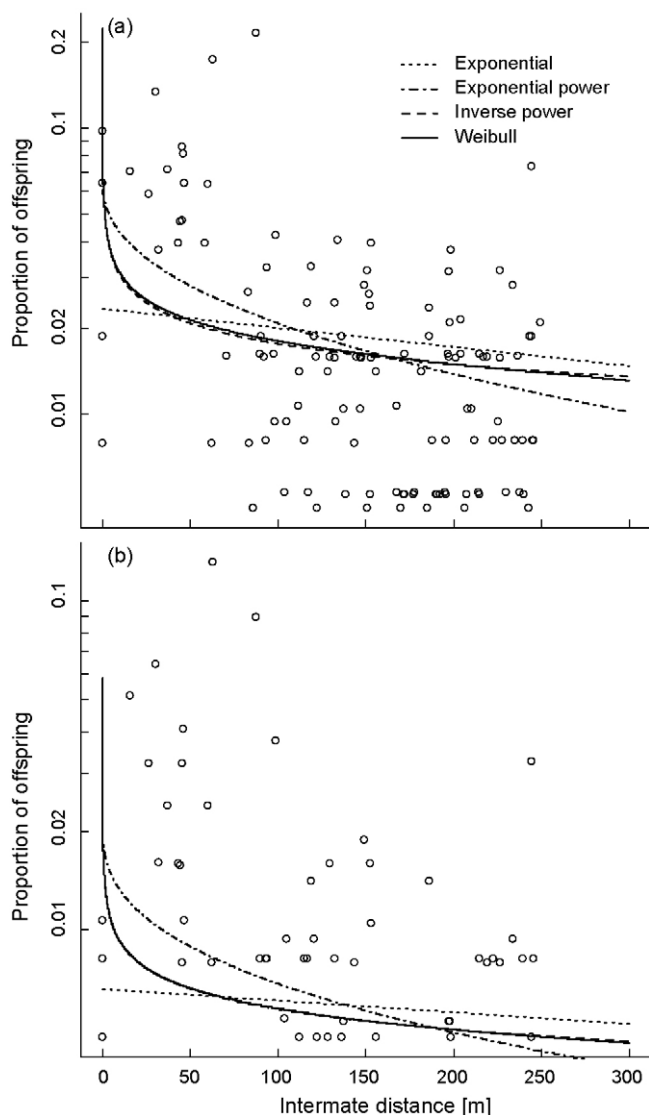
Fig. 4. (a and b) Pollen dispersal curves estimated with observed pollen dispersal distances (inter-mate distance) of five seed trees and modelled with the exponential, exponential power, inverse power, and Weibull functions. Datasets were generated with a paternity assignment based on the 80% (a) and 95% (b) confidence levels. Values on y-axis indicate the log 10-proportional contribution of a pollen donor out of total progeny per seed tree.

the individual maternal trees showed significant heterogeneity (values not reported). Thus, we found no evidence that pollen donors from the same quadrant as the canopy sector contributed disproportionately to paternity.

Pollen pool structure, estimated from TwoGENER analysis, also showed no meaningful 'quadrant effect' within seed trees

($\Phi_{QF} = 0.011$, $P > 0.25$; Table 4). Despite the relatively short distances among focal seed trees—some pairs were less than 200 m apart, the pollen pools differed significantly among seed trees ($\Phi_{FT} = 0.042$, $P < 0.01$; Table 4). Thus, seed trees received pollen from divergent arrays of paternal donors, but the pollen sources were sufficiently mixed within a single canopy that the entire canopy samples from the same pollen sources.

4. Discussion

4.1. Patterns of paternity

The pattern of paternity showed a highly skewed contribution of pollen sources, such that nearby sires were much more likely to fertilize offspring. In fact, the mean distance between seed trees and pollen donors who fertilized more than 10% of the assigned progeny was about 64 m, while the mean inter-mate distance of the pollen donors who fertilized only 1–2 offspring was 171 m, using the 80% CL dataset. The 25% nearest neighbours in the 20 ha plots accounted for more than half of the assigned siring events (55% and 65% for the 80% CL and the 95% CL, respectively), reflecting the over-representation of nearby pollen trees.

Our results concur with previous studies showing that domination of local pollen sources is the norm for wind-pollinated species. For example, Nakanishi et al. (2004) reported disproportionate fertilization of near-neighbour pollen sources for *Quercus salicina* within a 340 m × 340 m study plot. Streiff et al. (1999) reported a significant excess of pollinating parents within the first 20 m of the mother for 8 of 13 maternal trees in *Quercus robur* and *Quercus petrea*, relative to the proportion of potential pollen donors. Similarly, Dow and Ashley (1998) reported that 54% of all pollinations came from 20% of the candidate trees within 70 m in *Quercus macrocarpa* and Pakkard et al. (2008) reported that 72.8% of all pollinations came from candidate trees within 50 m to the seed trees in *Quercus semiserrata*. This propensity towards proximal mating in plant populations and a skewed contribution of individual pollen donors indicates the importance of the distribution and density of neighbouring adult trees, not ignoring the fact that all of these studies found significant pollen movement beyond 100 m as well.

Our estimate for pollen inflow in *Q. lobata* was 18.5% for the five focal trees, indicating moderate levels of pollen inflow from beyond 250 m. Because gene flow estimates depend on the size of the plot relative to adult density, comparisons across studies are always difficult. For example, in *Q. salicina*, about 44% of the pollinations occurred beyond 100 m for trees within a 11.56 ha plot (Nakanishi et al., 2005), which is a higher percentage inflow than we observed, but the size of the buffer is less than the size we used. In our study, this level of pollen inflow illustrates that the neighbouring trees outside the plot in this contiguous area of trees contribute to local matings, but we have captured a sufficient number of matings to assess the pattern of local matings.

Table 4
Hierarchical analysis of molecular variance (AMOVA) of pollen pools among seed source trees and among quadrants within canopies. See Section 2 for how genetic contributions of pollen donors were obtained.

Source of haplotypic variation	Degrees of freedom	Sum of squared deviations	Mean squared deviation	Expected mean squared deviations	Variance components	Φ
Among mothers	4	37.81	9.45	$\sigma_w^2 + k_2 \cdot \sigma_q^2 + k_3 \cdot \sigma_m^2$	4.17%[**]	$\Phi_{FT} = 0.042$
Among quadrants, within mothers	15	28.65	1.91	$\sigma_w^2 + k_1 \cdot \sigma_q^2$	1.04% ns	$\Phi_{QF} = 0.011$
Within quadrants	573	840.29	1.47	σ_w^2	94.79%	

ns = non-significant.
[**] $P < 0.01$.

The number of local contributing pollen donors is a critical determinant of the fine scale genetic structure of a population. In this study site, the number of available *Q. lobata* adults ranged from 30 to 38 trees per 20 ha plot, but the number of trees siring offspring was 20–32 trees for the 80% CL dataset (Table 2). When we estimate the average effective number of pollen donors per seed tree, we estimate 10.1 pollen donors per 250 m radius plot. This unequal contribution of local donors is what creates a genetic neighbourhood within a large continuously distributed population (Wright, 1943). The pollen pool structure approach through TwoGener procedure provides an estimate of the effective number of pollen donors for an idealized neighbourhood (Austerlitz and Smouse, 2001), which is an indication of the opportunity for population subdivision. The numbers of effective pollen donors estimated in this study via paternity analysis are within the same magnitude as other TwoGener estimates for *Q. lobata* in 2001 (N_{ep} = 12.5; Austerlitz et al., 2007), and for other oak species. For example, similar values were found in forest populations of *Q. alba* in Missouri (N_{ep} = 8.2, Smouse et al., 2001), *Q. velutina* in Missouri (N_{ep} = 7.5, Fernandez-Manjarrés et al., 2006), and *Q. humboldtii* in Colombia, South America (N_{ep} = 6.1, Fernandez and Sork, 2005). Pakkard et al. (2008) estimated approximately 18 and 7 effective pollen donors in a mast and non-mast year, respectively, of a low-density *Q. semiserrata* population (2.4 trees/ha) occurring in a former evergreen forest in Thailand. In general, the majority of oak studies report values of 12 or fewer effective pollen donors. Nonetheless the overall similarity of estimates of N_{ep} illustrates that that the paternity-based estimates based on a plot size that approximates a neighbourhood area are substitutable to those obtained for TwoGener based on the entire pollen pool and *vice versa*.

If we consider the Figueroa valley as a larger region, then the effective number of pollen donors will be much higher. Although we did not take measurements across the entire valley, if we pool the areas sampled by the five focal trees the overall N_{ep} increases. Due to overlap in the 20 ha plots, the pooled area is 58.9 ha, just under 60 ha. For the collection of five maternal trees, we estimated a pollen inflow adjusted N_{ep} of 56.9. It is a little difficult to use paternity analysis to estimate regional size of effective pollen donors because the regional estimate must take into account the extent to which different seed trees share the same pollen sources. For pollen inflow, we do not know the pollen sources and, without this precise information, the regional N_{ep} might be overestimated because it is likely to treat the same pollen source as new pollen sources across females. Nonetheless, this estimate of regional effective population size illustrates that larger contiguous regions will include more genetic variation. Thus, it is always a good rule of thumb that as the size of the local population increases, the overall N_{ep} will increase as well, whenever there is local population subdivision. When we are considering strategies for conservation of biodiversity, we want to measure effective number of pollen donors within neighbourhoods and the additional number for the larger stand.

4.2. Mean effective pollen dispersal distance

The unequal contribution of local pollen sources leads to effective mean pollen dispersal distances of 114 m within the 20 ha plot for the 80% CL, far below the median of all potential mating pairs of 167 m. Based on a pollen pool structure approach (TwoGener) at the same study site in 2001, Austerlitz et al. (2004) estimated average effective pollen dispersal distances for *Q. lobata* of 114, 121, and 129 m, for the exponential, exponential power, and Weibull functions, based on the observed adult density, respectively. Observed dispersal distances in the two studies yield similar values of effective dispersal distances, because estimates are heavily weighted by pollen donors that contribute most to the pollen pool. In a low-density population of *Q. semiserrata*, Pakkard et al. (2008) found similar values of dispersal distances: The average effective pollen dispersal distances were 109 and 68.3 m for a mast and a non-mast year, respectively. As long as the observed pollen dispersal distance for matings within a proscribed area includes a majority of the mating events, the dataset will yield a reasonable approximation of the effective dispersal distance, which – for *Q. lobata* – is on the order of 110 m.

4.3. Pollen dispersal models

The analysis of four dispersal curve functions indicated that three of the functions fit the data fairly well, and the exponential power model gave a slightly better fit. The exponential function provided the poorest fits for observed dispersal kernels of *Q. lobata* because it did not capture the steep decline of local dispersal. Our finding contrasts with that of Streiff et al. (1999), who concluded that the exponential function was a better fit than the exponential power for pollen dispersal data from two European oak species. Nakanishi et al. (2004) also used an exponential function to model pollen dispersal, but inspection of their figure raises the question whether one of the functions used here might not have yielded a better fit. Similarly, Lian et al. (2001) used the exponential function for wind-pollinated *Pinus densiflora* for pollen dispersal out to 330 m, but did not test alternative functions. Robledo-Arnuncio and Gil (2005) modelled the pollen dispersal curve out to 750 m for *Pinus sylvestris* with an exponential power function, based on an exhaustive consideration of 36 candidate pollen donors. Oddou-Muratorio et al. (2005) modelled pollen movement by insects of *Sorbus torminalis* population and found that the exponential power function provided a better fit than either the normal or exponential model. Even though the exponential power function is frequently used (e.g. Lian et al., 2001; Setsuko et al., 2007; de-Lucas et al., 2008), it is often difficult to distinguish among families of dispersal functions (Okubo and Levin, 1989), particularly where only SDD observations are available. A range of mathematic models describing dispersal with steep decay functions near the maternal parent are equally appropriate for our study and probably for others as well. All of them will capture the SDD processes due to the disproportionate genetic contribution of nearby pollen sources, and they differ only slightly in their description of SDD. In this study, results from the exponential power and inverse power functions suggested fat tails. Using the TwoGener approach, *Q. lobata* data from the 2001 season also fit an exponential power model with a fat tail (Austerlitz et al., 2004). In a similar manner, data reported here and data from 2001 (Austerlitz et al., 2004) could both fit a Weibull distribution, with a shape parameter that suggests a thin tail. The gene flow dispersal literature is showing that the exponential power function is a useful model, and our analysis favours this model as well. The choice of function may have dramatic differences for projections of the tail, but for SDD, the important conclusion is that the functions that capture the steep decay rate near the pollen source will be most accurate.

It seems logical that wind-pollinated plants in a study site with an open landscape and a predominant wind direction would be subject to strong directionality in pollen flow. Yet, the incorporation of directionality into our regression model improved the fit only slightly. We found this same result while examining anisotropy in a different year with more modest flower and acorn production (Austerlitz et al., 2007), suggesting that such results may not be unique to the year of the survey. Upon close review of the literature, only a few studies indicate an effect of wind direction on pollination. In a natural stand of *Pinus attenuata*, distance, directionality, and paternal tree size influenced mating success within 11 m radius plots (Burczyk et al., 1996). Similarly, in

a clonal seed orchard of *Pseudotsuga menziesii*, Burczyk and Prat (1997) found that distance, direction, fecundity, and phenology influenced siring success within 30 m radius plots. These studies report a small effect of directionality at distances very close to the seed tree, but distance is still the predominant factor. Austerlitz et al. (2007) point out that large numbers of progeny per seed sources are required to detect anisotropy, so the large numbers of progeny per tree in this study provide credible evidence that the pollen clouds are not shaped by the predominant wind direction.

Despite the good fit of the dispersal models, it is apparent that many observations do not lie precisely on the predicted lines (Fig. 4a and b) and we have dismissed the possibility that wind is the main explanation. Comparison of the mating patterns of individual trees shows high tree-to-tree variance in spatial arrangement of successful sires and their proportional contribution vary among the five focal trees (Fig. 3a–e). For example, seed tree no. 35 (Fig. 3b) had a large number of progeny sired by a pollen donor located directly west of the maternal tree, at the outer edge of the 250 m buffer. There is no other tree crown between the seed tree and this pollen source that could interfere with pollen flow. Thus landscape spatial structure may influence mating patterns and these may get averaged out as you increase the number of maternal trees in the sample, but it will not be easy to test for spatial array in a dispersal model. Nonetheless, from first approximations, the distance effect as described by rapidly decaying dispersal kernels provides a good model for this oak savannah landscape.

4.4. Pollen mixing within a canopy

Q. lobata trees can have crowns on the order of 30 m in diameter, which is a little less than half the distance to many near-neighbours. Given that other studies report siring of different pollen sources in different parts of a trees' canopy (e.g. Lian et al., 2001), it would not have been surprising to find that the different parts of the majestic canopies of *Q. lobata* sampled pollen from different source trees. However, our analysis of mating pairs based on paternity assignments and pollen pool structure that includes the outcome of all matings demonstrate that that pollen genotypes are relatively homogeneously distributed within these tree crowns. This finding combined with the lack of anisotropy in successful fertilization suggests that the local aerodynamics of pollen movement within the savannah landscape create a mixed pollen cloud. Such results are consistent with the work of Di-Giovanni and Kevan (1991) that shows that turbulence increases when forest canopies are open and uneven, which promotes and homogenizes pollen dispersal. In sum, the concern that different parts of the valley oak canopy sample different pollen donors can be dismissed.

4.5. Implications for sustainable management

The distribution and abundance of *Q. lobata* in California has been reduced and fragmented by agriculture and urban development, shrinking regional population size and isolating fragments. In addition, many remnant valley oak woodlands and savannahs are thinning, due to a lack of new recruits. Because this species is in jeopardy from ongoing landscape transformation, state and local policies have been designed to promote oak conservation and mitigate impacts of development and agricultural activities (a summary of county policies is available from the University of California's integrated hardwood range management program, http://danr.ucop.edu/ihrmp/county/). Twenty counties have passed ordinances requiring the establishment of new oaks to offset permitted removals and a few go as far as specifying that seeds should be obtained "from local sources". Mitigation actions tend to be project-specific and there is little attention to cumulative local or landscape-scale effects of oak removal or re-planting on population viability or genetic connectivity.

Our results, along with those from previous work (Sork et al., 2002b; Austerlitz et al., 2004, 2007) provide some guidance on how to maintain the long-term viability of valley oak, in the face of ongoing development and other environmental changes. First, we see that the effective number of pollen donors for single *Q. lobata* adults is substantially lower than the adult population size and that effective dispersal distance is on the order of 110 m. Given the localized nature of both pollen and acorn dispersal, combined with progressively decimated populations, increasing population sub-division and genetic drift are probable (see Aguilar et al., 2008). Because genetic variation enhances the ability of populations to respond to environmental change, management practices that preserve gene flow processes should be promoted and ordinances that require use of local seed sources should not be so restrictive in their definition of local that gene flow is restricted. Second, given the importance of near-neighbours to the local pollen pool, our results suggest that it would be far better to preserve clusters of trees that can contribute to a large local pollen pool, rather than allow tree removals that result in hyper-dispersion of adults, where a single near-neighbour could dominate a pollen pool. Pollen flow is key to maintaining genetic variation, and the spatial array of trees will have an important impact. Finally, we want to point out that our goal here is not to discount the importance of connectivity among local populations because LDD is a source of genetic variation for local populations. Instead, we focus on SDD to emphasize that management of natural tree populations should pay attention to these local processes because they produce the immediate source of genetic variation influencing short-term ecological and evolutionary processes that are affected by land-scape and climate changes.

Appendix A. Supplementary data

Supplementary data associated with this article can be found, in the online version, at doi:10.1016/j.foreco.2009.05.014.

References

Adams, W., Birkes, D., 1991. Estimating mating patterns in forest tree populations. In: Fineschi, S., Malvolti, M., Cannata, F., Hattemer, H. (Eds.), Biochemical Markers in the Population Genetics of Forest Trees. SBP Academic, The Hague.

Aguilar, R., Quesada, M., Ashworth, L., Herrerias-Diego, Y., Lobo, J., 2008. Genetic consequences of habitat fragmentation in plant populations: susceptible signals in plant traits and methodological approaches. Molecular Ecology 17, 5177–5188.

Akaike, H., 1974. New look at statistical-model identification. IEEE Transactions on Automatic Control AC19 716–723.

Austerlitz, F., Smouse, P., 2001. Two-generation analysis of pollen flow across a landscape. II. Relation between Phi(ft), pollen dispersal and interfemale distance. Genetics 157, 851–857.

Austerlitz, F., Dick, C., Dutech, C., Klein, E., Oddou-Muratorio, S., Smouse, P., Sork, V., 2004. Using genetic markers to estimate the pollen dispersal curve. Molecular Ecology 13, 937–954.

Austerlitz, F., Dutech, C., Smouse, P.E., Davis, F., Sork, V.L., 2007. Estimating aniso-tropic pollen dispersal: a case study in *Quercus lobata*. Heredity 99, 193–204.

Bates, D.M., Watts, D.G., 1988. Nonlinear Regression Analysis and Its Applications. Wiley, New York, United States.

Bates, D.M., Chambers, J.M., 1992. Nonlinear models. In: Chambers, J.M., Hastie, T.J. (Eds.), Statistical Models in S. Wadsworth & Brooks/Cole. Pacific Grove (CA), United States.

Burczyk, J., Adams, W., Shimizu, J., 1996. Mating patterns and pollen dispersal in a natural knobcone pine (*Pinus attenuata* Lemmon) stand. Heredity 77, 251–260.

Burczyk, J., Prat, D., 1997. Male reproductive success in *Pseudotsuga menziesii* (Mirb) France: the effects of spatial structure and flowering characteristics. Heredity 79, 638–647.

Burczyk, J., Adams, W., Moran, G., Griffin, A., 2002. Complex patterns of mating revealed in a *Eucalyptus regnans* seed orchard using allozyme markers and the neighbourhood model. Molecular Ecology 11, 2379–2391.

Burczyk, J., Lewandowski, A., Chalupka, W., 2004. Local pollen dispersal and distant gene flow in Norway spruce (*Picea abies* LKarst.). Forest Ecology and Management 197, 39–48.

Cain, M.L., Nathan, R., Levin, S.A., 2003. Long-distance dispersal. Ecology 84, 1943–1944.

Clark, J., 1998. Why trees migrate so fast: confronting theory with dispersal biology and the paleorecord. American Naturalist 152, 204–224.

Clark, J.S., Silman, M., Kern, R., Macklin, E., HilleRisLambers, J., 1999. Seed dispersal near and far: patterns across temperate and tropical forests. Ecology 80, 1475–1494.

de-Lucas, A.I., Robledo-Arnuncio, J.J., Hidalgo, E., Gonzalez-Martinez, S.C., 2008. Mating systems and pollen gene glow in Mediterranean maritime pine. Heredity 100, 390–399.

Di-Giovanni, F., Kevan, P., 1991. Factors affecting pollen dynamics and its impor-tance to pollen contamination—a review. Canadian Journal of Forest Research-Revue Canadienne De Recherche Forestiere 21, 1155–1170.

Di-Giovanni, F., Kevan, P., Arnold, J., 1996. Lower planetary boundary layer profiles of atmospheric conifer pollen above a seed orchard in northern Ontario Canada. Forest Ecology and Management 83, 87–97.

Dow, B., Ashley, M., Howe, H., 1995. Characterization of highly variable (GA/CT)(n) microsatellites in the Bur Oak, *Quercus macrocarpa*. Theoretical and Applied Genetics 91, 137–141.

Dow, B., Ashley, M., 1998. Factors influencing male mating success in bur oak, *Quercus macrocarpa*. New Forests 15, 161–180.

Fernandez, J.F., Sork, V.L., 2005. Mating patterns of a subdivided population of the Andean oak (*Quercus humboldtii* Bonpl., Fagaceae). Journal of Heredity 96, 635–643.

Fernandez-Manjarrés, J., Idol, J., Sork, V.L., 2006. Mating patterns of black oak *Quercus velutina* (Fagaceae) in a Missouri Oak-Hickory Forest. Journal of Her-edity 97, 451–455.

Gregory, P., 1968. Interpreting plant disease dispersal gradients. Annual Review of Phytopathology 6, 189–212.

Kampfer, S., Lexer, C., Glossl, J., Steinkellner, H., 1998. Characterization of (GA)(n) microsatellite loci from *Quercus robur*. Hereditas 129, 183–186.

Kelly, P.A., Phillips, S.E., Williams, D.F., 2005. Documenting ecological change in time and space: The San Joaquin Valley of California. In: Lacey, E.A., Myers, P. (Eds.), Mammalian Diversification: From Chromosomes to Phylogeography. University of California Publications in Zoology, California, pp. 57–78.

Klein, E.K., Lavigne, C., Picault, H., Michel, R., Gouyon, P.H., 2006. Pollen dispersal of oilseed rape: estimation of the dispersal function and effects of field dimension. Journal of Applied Ecology 43, 141–151.

Lian, C., Miwa, M., Hogetsu, T., 2001. Outcrossing and paternity analysis of *Pinus densiflora* (Japanese red pine) by microsatellite polymorphism. Heredity 87, 88–98.

Mahall, B.E., Davis, F.W., Tyler, C.M., 2005. Final report of the Santa Barbara County Oak Restoration Program: August 1994–August 2005. County of Santa Barbara Department of Planning and Development, Energy Division, University of California Santa Barbara.

Marshall, T., Slate, J., Kruuk, L., Pemberton, J., 1998. Statistical confidence for likelihood-based paternity inference in natural populations. Molecular Ecology 7, 639–655.

Meagher, T., 1986. Analysis of paternity within a natural-population of *Chamaelir-ium luteum* 1. Identification of most-likely male parents. American Naturalist 128, 199–215.

Nakanishi, A., Tomaru, N., Yoshimaru, H., Kawahara, T., Manabe, T., Yamamoto, S., 2004. Patterns of pollen flow and genetic differentiation among pollen pools in *Quercus salicina* in a warm temperate old-growth evergreen broad-leaved forest. Silvae Genetica 53, 258–264.

Nakanishi, A., Tomaru, N., Yoshimaru, H., Manabe, T., Yamamoto, S., 2005. Inter-annual genetic heterogeneity of pollen pools accepted by *Quercus salicina* individuals. Molecular Ecology 14, 4469–4478.

Nathan, R., Muller-Landau, H.C., 2000. Spatial patterns of seed dispersal, their determinants and consequences for recruitment. Trends in Ecology & Evolution 15, 278–285.

Nathan, R., Perry, G., Cronin, J., Strand, A., Cain, M., 2003. Methods for estimating long-distance dispersal. Oikos 103, 261–273.

Nielsen, D.I., Tarpy, D.R., Reeve, H.K., 2003. Estimating effective paternity number in social insects and the effective number of alleles in a population. Molecular Ecology 12, 3157–3164.

Oddou-Muratorio, S., Houot, M., Demesure-Musch, B., Austerlitz, F., 2003. Pollen flow in the wildservice tree, *Sorbus torminalis* (L.) Crantz I. Evaluating the paternity analysis procedure in continuous populations. Molecular Ecology 12, 3427–3439.

Oddou-Muratorio, S., Klein, E., Austerlitz, F., 2005. Pollen flow in the wildservice tree, *Sorbus torminalis* (L.) Crantz II. Pollen dispersal and heterogeneity in mating success inferred from parent-offspring analysis. Molecular Ecology 14, 4441–4452.

Ogden, G., 1975. Differential response of two oak species to far inland advection of sea-salt spray aerosol. Ph.D. dissertation. University of California, Santa Barbara, CA, USA.

Okubo, A., Levin, S., 1989. A theoretical framework for data-analysis of wind dispersal of seeds and pollen. Ecology 70, 329–338.

Pakkard, G., Ueno, S., Yoshimaru, H., 2008. Gene flow pattern and mating system in a small population of *Quercus semiserrata* Roxb (Fagaceae). Forest Ecology and Management 225, 3819–3826.

Pavlik, B., Muick, P., Johnson, S., Popper, M., 1991. Oaks of California. In: Cashuma Press and The California Oak Foundation, Los Olivos, CA, USA.

Robledo-Arnuncio, J., Gil, L., 2005. Patterns of pollen dispersal in a small population of *Pinus sylvestris* L. revealed by total-exclusion paternity analysis. Heredity 94, 13–22.

Robledo-Arnuncio, J.J., Garcia, C., 2007. Estimation of the seed dispersal kernel from exact identification of source plants. Molecular Ecology 16, 5098–5109.

Setsuko, S., Ishida, K., Ueno, S., Tsumura, Y., Tomaru, N., 2007. Population differ-entiation and gene flow within a metapopulation of a threatened tree, *Magnolia stellata* (Magnoliaceae). American Journal of Botany 94, 128–136.

Shen, H., Rudin, D., Lindgren, D., 1981. Study of the pollination pattern in a Scots pine seed orchard by means of isoenzyme analysis. Silvae Genetica 30, 7–15.

Slavov, G.T., Howe, G.T., Gyaourova, A.V., Birkes, D.S., Adams, W.T., 2005. Estimating pollen flow using SSR markers and paternity exclusion: accounting for mis-typing. Molecular Ecology 14, 3109–3121.

Smouse, P., Dyer, R., Westfall, R., Sork, V., 2001. Two-generation analysis of pollen flow across a landscape I. Male gamete heterogeneity among females. Evolution 55, 260–271.

Sork, V., Davis, F., Dyer, R., Smouse, P., 2002. Mating patterns in a Savanna popula-tion of Valley oak (*Quercus lobata* Nee). In: Standiford, R., McCreary, D., Purcell, K. (Eds.), Fifth Symposium on Oak Woodlands: Oaks in California's Changing Landscape, 22–25 October 2001, USDA Forest Service General Technical Report, PSW-GTR-184, San Diego, CA, USA, pp. 427–439.

Sork, V., Davis, F., Smouse, P., Apsit, V., Dyer, R., Fernandez, J., Kuhn, B., 2002b. Pollen movement in declining populations of California Valley oak, *Quercus lobata*: where have all the fathers gone? Molecular Ecology 11, 1657–1668.

Sork, V.L., Smouse, P.E., 2006. Genetic analysis of landscape connectivity in tree populations. Landscape Ecology 21, 821–836.

Steinkellner, H., Fluch, S., Turetschek, E., Lexer, C., Streiff, R., Kremer, A., Burg, K., Glossl, J., 1997. Identification and characterization of (GA/CT)(n)-microsatellite loci from *Quercus petraea*. Plant Molecular Biology 33, 1093–1096.

Streiff, R., Ducousso, A., Lexer, C., Steinkellner, H., Gloessl, J., Kremer, A., 1999. Pollen dispersal inferred from paternity analysis in a mixed oak stand of *Quercus robur* L and *Q. petraea* (Matt) Liebl. Molecular Ecology 8, 831–841.

Tufto, J., Engen, S., Hindar, K., 1997. Stochastic dispersal processes in plant popula-tions. Theoretical Population Biology 52, 16–26.

Tyler, C.M., 2006. Demography and recruitment limitations of three oak species in California. The Quarterly Review of Biology 81, 127–152.

Venables, W.N., Ripley, B.D., 2002. Modern Applied Statistics with S. Springer, New York.

Westneat, D.F., Webster, M.S., 1994. Molecular analysis of kinship in birds: inter-esting questions and useful techniques. In: Schierwater, B., Streit, B., Wagner, G.P., Desalle, R. (Eds.), Molecular Ecology and Evolution: Approaches and Applications. Birkhaeuser Verlag, Basel, Switzerland.

Weibull, W., 1951. A statistical distribution function of wide applicability. Journal of Applied Mechanics-Transactions of the ASME 18, 293–297.

Wingen, L.U., Brown, J.K.M., Shaw, M.W., 2007. The population genetic structure of clonal organisms generated by exponentially bounded and fat-tailed dispersal. Genetics 177, 435–448.

Wright, S., 1943. Isolation by distance. Genetics 28, 114–138.

Wright, S., 1946. Isolation by distance under diverse systems of mating. Genetics 31, 39–59.